Reduction-Induced Inhibition and Mn(II) Release from the Photosystem II Oxygen-Evolving Complex by Hydroquinone or NH_2OH Are Consistent with a Mn(III)/Mn(III)/Mn(IV)/Mn(IV) Oxidation State for the Dark-Adapted Enzyme[†]

Thomas Kuntzleman and Charles F. Yocum*

Department of Molecular, Cellular and Developmental Biology and Department of Chemistry, University of Michigan, Ann Arbor, Michigan 48109-1048

Received July 19, 2004; Revised Manuscript Received November 24, 2004

ABSTRACT: Hydroxylamine and hydroquinone were used to probe the oxidation states of Mn in the oxygen-evolving complex of dark-adapted intact (hydroxylamine) and salt-washed (hydroquinone) photosystem II. These preparations were incubated in the dark for 24 h in the presence of increasing reductant/photosystem II ratios, and the loss of oxygen evolution activity and of Mn(II) was determined for each incubation mixture. Monte Carlo simulations of these data yielded models that provide insight into the structure, reactivity, and oxidation states of the manganese in the oxygen-evolving complex. Specifically, the data support oxidation states of $Mn(III)_2/Mn(IV)_2$ for the dark stable S_1 state of the O_2-evolving complex. Activity and Mn(II) loss data were best modeled by assuming an $S_1 \rightarrow S_{-1}$ conversion of intermediate probability, a $S_{-1} \rightarrow S_{-3}$ reaction of high probability, and subsequent step(s) of low probability. This model predicts that photosystem II Mn clusters that have undergone an initial reduction step become more reactive toward a second reduction, followed by a slower third reduction step. Analysis of the Mn-(II) release parameters used to model the data suggests that the photosystem II manganese cluster consists of three Mn atoms that exhibit a facile reactivity with both reductants, and a single Mn that is reducible but sterically trapped at or near its binding site. Activity assays indicate that intact photosystem II centers reduced to S_{-1} can evolve oxygen upon illumination, but that these centers are inactive in preparations depleted of the extrinsic 23 and 17 kDa polypeptides. Finally, it was found that a substantial population of the tyrosine D radical is reduced by hydroxylamine, but a smaller population reacts with hydroquinone over the course of a 24 h exposure to the reductant.

Photosystem II (PSII), a membrane-bound pigment−protein complex, uses light energy to catalyze water oxidation (*1*, *2*): $2H_2O \rightarrow 4\ H^+ + 4e^- + O_2$

Photons absorbed by PSII initiate a series of redox reactions that culminate in the sequential oxidation of the oxygen-evolving complex (OEC).[1] The OEC consists, in part, of a cluster of inorganic ions (4Mn, Ca^{2+}, and Cl^-) that cycle through 5 oxidation states, as described by the Kok model (*3*, *4*):

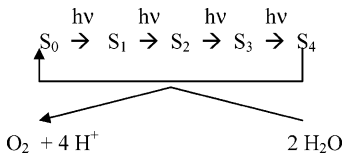

Once the S_4 state is reached, O_2 is released and the cluster is reduced to the S_0 state. It is generally agreed that one oxidizing equivalent separates the S_0/S_1 and the S_1/S_2 states (*2*), and that these S-state transitions consist of oxidations of the Mn atoms in the cluster. However, generation of S_3 has been postulated to occur by oxidation either of the Mn cluster, of a substrate ligand, or of a redox-active tyrosine residue (Y_Z) (*2*). Upon long-term (> 30 min) dark incubation, all PSII centers relax to the S_1 state (*3*, *4*).

Calcium and chloride cofactors, as well as Y_Z, are required for the redox reactions leading to water oxidation (*1*, *2*). Binding of these cofactors is regulated by extrinsic 23 and 17 kDa polypeptides (*5*−*7*), and perhaps also by intrinsic polypeptides of the PSII reaction center (*8*). These polypeptides and Y_Z are also components of the OEC. It is generally agreed that water binds directly to the Mn atoms and perhaps Ca^{2+} in the OEC, but the S-state(s) to which water(s) bind is still under investigation. In addition to Y_Z, there is a second redox active tyrosine (Y_D) that does not participate in oxygen

[†] This research was supported by grants to C.F.Y. from the United States Department of Agriculture National Research Initiative Competitive Research Grants Program and the Molecular Biochemistry Program of NSF. T.K. was supported by a Molecular Biophysics Training Grant from the NIH.

* To whom correspondence should be addressed: Department of Molecular, Cellular and Developmental Biology, University of Michigan, Ann Arbor, MI 48109-1048. Tel: 1-734-647-0897. Fax: 1-734-647-0884.

[1] Abbreviations: Chl, chlorophyll; DCBQ, 2,6-dichloro-*p*-benzoquinone; EDTA, ethylenediamine tetraacetic acid; H_2Q, hydroquinone; MES, 2-(*N*-morpholino)ethanesulfonic acid; OEC, O_2-evolving complex; PS, photosystem; MC, buffer composed of 50 mM MES (pH 6) and 10 mM $CaCl_2$; SMN, buffer composed of sucrose (0.4 M), MES (50 mM, pH 6), 10 mM NaCl); SWPSII, photosystem II preparation treated with 2 M NaCl to extract Ca^{2+} and the 23 and 17 kDa extrinsic polypeptides; XANES, X-ray absorption near edge spectroscopy, $Y_D^{\bullet}$, a dark-stable tyrosine radical (Y160 of the PsbD protein) of photosystem II.

10.1021/bi048460i CCC: $30.25
Published on Web 01/19/2005

evolution. It is present as a dark stable radical, $Y_D^{\bullet}$, in a large percentage of PSII centers, and is detectable by EPR spectroscopy (*9*).

Because it is relatively easy to achieve high concentrations of PSII centers trapped in S_1 or S_2, there is a large body of information on these two states of the enzyme. X-ray absorption near edge structure (XANES) and EPR spectroscopies have provided useful information on the probable oxidation states of the Mn cluster in S_1 and S_2 (*10*−*17*). Results of XANES experiments on S_1 are interpreted to support an oxidation state composed of $Mn(III)_2Mn(IV)_2$ (*10*, *11*). However, an alternate model proposes cluster oxidation states of $Mn(III)_4$, which would yield an S_2 oxidation state of $Mn(III)_3Mn(IV)$. This predicted oxidation state provides an excellent basis for modeling the features of the multiline EPR signal (*17*) associated with S_2. This signal, formed by illumination of dark-adapted PSII centers at 195 K, is centered at $g \approx 2.0$ and is characterized by multiple lines (>16) that span ca. 1400−1600 G (*12*). The multiline signal has been simulated by assigning the S_2 Mn oxidation states as either $Mn(III)_3Mn(IV)$ (*13*, *14*) or $Mn(III)Mn(IV)_3$ (*15*, *16*). Since a single turnover of the OEC advances the S_1 state to S_2, only the latter oxidation state model is consistent with the S_1 state XANES results. Additional data would help to unambiguously assign oxidation states of the Mn cluster in each step of the Kok cycle, and contribute to a better understanding of the mechanism of water oxidation.

Reductants such as hydroxylamine (NH_2OH) or hydroquinone (H_2Q) have proved to be useful probes of the reactivity of the OEC Mn cluster and its oxidation states. Under conditions of short-term exposure, and at low (μM) concentrations, NH_2OH has been demonstrated to reversibly reduce the OEC, producing states S_0, S_{-1}, and S_{-3}. XANES experiments have shown that the Mn cluster of PSII centers incubated with low concentrations of NH_2OH has an oxidation state of $Mn(III)_4$ (*11*), which is consistent with the existence of a $Mn(III)_2Mn(IV)_2$ S_1 oxidation state that has been reduced by two electrons. At high (mM) concentrations, NH_2OH inactivates the enzyme irreversibly, simultaneously extracting 3−4 Mn(II) from each PSII center (*18*, *19*). Incubation of thylakoid membranes with low NH_2OH concentrations delays the appearance of O_2 by 2 flashes; O_2 release occurs on the 5th, rather than the 3rd, flash (*20*). A two-step delay in the normal flash-induced proton release pattern was also detected (*21*, *22*) in experiments on thylakoid membranes treated with NH_2OH. Although NH_2OH is a one-electron reductant, these results suggest that it catalyzes a two-electron reduction of the Mn cluster, which produces the stable S_{-1} state. A variety of experimental reports support this conclusion (*20*−*25*). Formation of an S_0 state and its associated multiline signal in NH_2OH-treated samples (*26*, *27*) would imply that this state is an intermediate in the reduction of S_1 to S_{-1} as well as in the oxidation of S_{-1} to S_1.

In addition to NH_2OH, other small molecules such as hydrazine (N_2H_4) and $NO^{\bullet}$ have been used to produce high concentrations of reduced PSII centers in non-native oxidation states (*22*, *28*, *29*). Flash-induced oscillatory patterns of PSII centers treated with $NO^{\bullet}$ or N_2H_4 exhibit a three or four flash delay in the onset of O_2 evolution, indicating that S_{-2} and S_{-3} states have been formed by these reductants. In the case of $NO^{\bullet}$, a multiline EPR spectrum assigned to the Mn cluster in the S_{-2} state has been observed. Indirect evidence from simulations of the flash oscillation patterns in these studies points to centers reduced as low as S_{-4} and S_{-5}. If these assignments are correct and are due solely to Mn reduction, this would favor a $Mn(III)_2Mn(IV)_2$ S_1 oxidation state.

The extrinsic 23 and 17 kDa polypeptides must be extracted in order for the bulkier reductant H_2Q to access and reduce the Mn cluster (*30*, *31*). After reconstitution with Ca^{2+}, H_2Q reduction of these salt-washed PSII centers has been shown by XANES spectroscopy to yield a Mn cluster containing a putative S_{-1} state ($Mn(II)_2Mn(IV)_2$) that is distinct from the S_{-1} state formed by treatment with NH_2OH ($Mn(III)_4$). Furthermore, H_2Q-treated salt-washed PSII centers retained high levels of activity and exhibited a Mn(II) six-line EPR signal at 25 °C whose intensity corresponded to about 50% of the total Mn population (*11*). This signal was diminished significantly upon illumination (*30*). Both of these experiments suggest that the Mn oxidation states in S_1 are $Mn(III)_2Mn(IV)_2$. Taken together, the NH_2OH and H_2Q studies provide insight into the reactivity of the Mn cluster. For example, the different Mn oxidation states detected in the S_{-1} state depended upon the reductant used, which implies that the two reductants must react at different sites in the cluster in order to generate the different S_{-1} states detected by XANES. Separate sites of reaction with these reductants is in agreement with the observation that PSII centers incubated simultaneously for short periods of time with noninhibitory concentrations of both NH_2OH and H_2Q were rapidly inactivated (*30*), which suggests that the two reductants react synergistically with the Mn cluster.

No experiments have addressed the stoichiometry of the reaction between the PSII Mn cluster and exogenous reductants. In the experiments presented here, end-point titrations were performed on PSII preparations exposed to stoichiometric amounts of NH_2OH (intact) and H_2Q (salt-washed). The losses of activity and of Mn(II) were analyzed in order to determine the number of oxidizing equivalents stored in the S_1 state. This chemical information, in conjunction with prior EPR and XANES data (*11*, *15*, *32*−*34*), provides strong evidence for a $Mn(III)_2Mn(IV)_2$ oxidation state assignment of the Mn cluster in S_1. In addition, these data also suggest that reduction of the Mn cluster is most likely to occur by a mechanism in which centers that have undergone an initial reduction step are more sensitive to succeeding reduction reactions. Furthermore, at least some reduced centers are metastable with respect to Mn ligation; they are able to photoactivate and evolve O_2 upon illumination, but lose Mn(II) and activity upon exposure to high Ca^{2+} concentrations in the dark.

MATERIALS AND METHODS

Sample Preparation. Isolated PSII was prepared from market spinach using the method of Berthold et al. (*35*) with the modifications described in Ghanotakis et al. (*31*). Extraction of the 17 and 23 kDa polypeptides was accomplished by incubating PSII membranes for 1 h in 2 M NaCl at 0 °C. Salt-washed samples were washed twice in a buffer containing 400 mM sucrose, 50 mM MES, and 10 mM NaCl at pH 6.0 (SMN buffer). Mn depleted PSII

membranes were prepared by incubating salt-washed PSII membranes in 1 mM NH_2OH for 1 h, centrifuging at 12000*g* for 20 min, and then washing and resuspending the resulting pellets twice in SMN. All PSII samples were stored in SMN (2−3 mg chlorophyll/mL) at −70 °C.

Activity Inhibition and O_2 Evolution Assays. Samples were thawed and placed on ice in the dark. If EDTA or Ca^{2+} was present during incubation experiments, it was added from a 0.1 M stock solution of the chelator, or from a freshly prepared 0.1 M $Ca(MES)_2$ solution. Stoichiometric amounts of NH_2OH or H_2Q (0.25−12 mol of reductant/mol of PSII, 250 Chl/PSII (*31*)) were added to 100 μL aliquots of the resulting PSII suspension (1.5−3 mg Chl/ml). The stock concentrations of reductants were 100 μM or 1 mM NH_2OH/H_2SO_4 or stock solutions of 100 μM or 1 mM H_2Q in ethanol. The reaction mixtures were incubated in the dark at 4−8 °C for 20−24 h. Results from 48 h incubations gave essentially the same results as 24 h incubations, indicating that the reactions were complete after 24 h. After incubation, aliquots from incubation mixtures were diluted 100−150-fold into a buffer containing 50 mM MES (pH 6) and 10 mM $CaCl_2$ (MC buffer) and assayed for activity at 25 °C using a Clark-type O_2 electrode with 350 μM DCBQ as the electron acceptor. Intact PSII preparations gave an activity of 600−700 μmol of O_2 mg chl^{-1} h^{-1}; salt-washed membranes assayed in MC buffer had activities of 300−400 μmol of O_2 mg chl^{-1} h^{-1}. The control sample for these experiments was a sample that was incubated without reductant overnight under the same conditions. These samples routinely showed <10% loss in activity (and <10% loss in Mn content, see below). The fraction of centers inactivated was assumed to fit the following equation:

$$F_I = \frac{A_C - A_R}{A_C}$$

where F_I is the fraction of centers inactivated, A_C is the activity of a sample incubated overnight in the absence of reductant, and A_R is the activity of a sample incubated overnight in the presence of reductant. In separate experiments, samples were treated as above, except that, after the 20−24 h incubation, 50 mM Ca^{2+} (as $CaCl_2$) was added to displace adventitiously bound Mn(II) (*19*). These samples were incubated in the presence of Ca^{2+} for an additional 30−60 min before assaying O_2 evolution as described above. Because these incubations were carried out aerobically, catalase was included in incubation mixtures to determine whether peroxide formation might occur as a side reaction during reduction of PSII Mn. Additions of saturating amounts of bovine liver catalase (Sigma, 1 mg/mL) to incubation mixtures had no effect on the reductant stoichiometries reported here, although it should be noted that NH_2OH is an inhibitor of the enzyme (*36*). At the concentrations of enzyme and NH_2OH used in these controls, we estimate that catalase activity ranged between 90% and 10% in these incubation controls, which would be sufficient to remove small (μM) amounts of H_2O_2, if it is in fact produced by the reductants.

Reductant Stability. Purification of the PSII samples used in these experiments employs EDTA during thylakoid isolation to sequester trace ions, including transition metals, which might otherwise give misleading results in the reductant studies reported here. The long-term stability of NH_2OH in SMN at 4 °C was tested by adding NH_2OH from a freshly prepared stock solution of 1 mM NH_2OH/H_2SO_4 to SMN buffer. The final concentrations were 10−20 μM NH_2OH, and the samples were incubated at 4−8 °C for 24 h in darkness. After 24 h, a set of fresh NH_2OH standards was prepared (10−50 μM) from a stock solution of 1 mM NH_2OH/H_2SO_4 in SMN. Next, *p*-nitrobenzaldehyde was added to each sample and they were analyzed as described by Johnson to determine NH_2OH concentrations (*37*). Using this analytical method, the samples incubated overnight showed no loss of NH_2OH relative to freshly prepared samples. The stability of NH_2OH upon incubation with PSII is described in "Results". The stability of H_2Q in SMN at 4 °C was determined by preparing solutions of 15−45 μM H_2Q in SMN using an ethanolic stock of 1 mM H_2Q. These samples were incubated at 4 °C for up to 5 days in darkness. After this time, the absorbance spectrum (200−400 nm) of each sample was taken and compared to the absorbance spectrum of freshly prepared 36 μM H_2Q and 36 μM H_2Q oxidized with ammonium persulfate (APS). No significant oxidation of H_2Q was detected in the absence of APS. Furthermore, PSII samples depleted of manganese (1 h treatment in 1 mM NH_2OH, followed by washing to remove reductant, which leaves the extrinsic polypeptides intact) and then incubated with 45 μM H_2Q in darkness for 24 h at 4 °C showed no evidence of H_2Q oxidation, which indicates that apo-PSII prepared by NH_2OH-catalyzed Mn^{2+} extraction does not oxidize H_2Q.

Quantification of Mn Loss from PSII. PSII membranes (300 μL aliquots) were prepared as described above. After incubation for 24 h under various conditions, the samples were centrifuged at 12000*g* for 20 min. The supernatant was decanted, and any residual liquid was removed with an absorbant tissue; special care was taken to remove any traces of supernatant while maintaining the integrity of the pellet. The pellets were then resuspended to their original 300 μL volume with 0.6 M HCl. Samples were placed in an aqueous flat cell, and Mn(II) 6-line EPR signals were measured at room temperature using a Bruker EMX spectrometer fitted with a TM cavity operated at X-band. Each sample was scanned once using the following instrument settings: power, 200 mW; modulation amplitude, 10 Gpp; and modulation frequency, 100 kHz. The sweep width was 900 G, the time constant was 10 ms, and center field was set at 3480 G. The Mn(II) concentration of each sample was determined by comparing the signal amplitudes to a set of standard Mn(II) solutions (5−100 μM) in 0.6 M HCl. The fraction of Mn remaining in a pellet was determined by comparing the average signal amplitude of a reductant treated sample to a control sample incubated without reductant. Typically, samples with no added reductant incubated overnight at 4−8 °C and then acidified showed a less than 10% loss of Mn relative to a sample that was acidified immediately after thawing. In separate experiments, 50 mM Ca^{2+} was added to reduced samples to release adventitiously bound Mn(II) as described above, prior to the centrifugation and acidification steps.

Measurement of $Y_D^{\bullet}$ EPR Signals. PSII membranes (300 μL aliquots) were treated with reductants as described above. After a 24 h incubation period, 1 mM EDTA was added

from a 0.1 M EDTA stock solution to suppress Mn(II) six-line signals. The $Y_D^{\bullet}$ signal amplitudes were determined at room temperature as described above, by measuring the peak-to-baseline signal height of the low field peak at ca. 3475 G. Each signal was scanned 4 times using the following instrument settings: power, 20 mW; modulation amplitude, 4 Gpp; and modulation frequency, 100 kHz. The sweep width was 100 G, the time constant was 164 ms, and center field was 3480 G.

Simulations. The O_2 Evolution and Mn extraction data were simulated using programs written in Mathcad 2001i, to generate models consistent with the experimental results. It was assumed that an irreversible reaction between PSII centers and the reducing agent occurred. The goal in extracting data from the end-point titrations was to determine the relative populations of each PSII state that resulted from the reaction of a particular reductant/PSII ratio. In each case, a specified number of reductant molecules (either 1 or 2) were assumed to react with a PSII center starting out in the S_1 state. Therefore, given a single reductant molecule (or two reductant molecules, in the case of model 3 below) and an ensemble of PSII centers in a variety of states, $PSII_n$, the probability that a PSII center in a particular PSII state, $PSII_n$, will react with the reductant molecule is proportional to the number molecules in the state $PSII_n$:

$$P_n \propto k_n[\text{number of PSII}_n\text{ molecules}]/\text{PSII}_{\text{tot}}$$

P_n is the probability that a state $PSII_n$ will react with reductant, $PSII_{tot}$ is the total number of PSII centers, and k_n is a weighted factor, specific to the state $PSII_n$, that takes into account the likelihood that the state $PSII_n$ will react relative to other states. This factor, although not a rate constant, should be largely dependent upon the rate of the reaction between the reductant and the state $PSII_n$, and should reflect the reactivity of each state toward the reductant. For these simulations, k_n was set equal to 1 for the most likely reaction in the sequence, and equal to fractions of 1 for reactions that were less likely to occur. Therefore, on the basis of these assumptions,

$$P_n = k_n[\text{number of PSII}_n\text{ molecules}]/\text{PSII}_{\text{tot}}$$

where P_n is the probability that a reaction between a PSII center in a specific state and a reductant molecule will occur.

On this basis, Monte Carlo simulations were run with the following initial parameters: 10000 molecules of PSII in the S_1 state, 0 molecules in reduced states, and saturating amounts of reductant. Each cycle involved the addition of incremental (1 H_2Q or 2 NH_2OH) amounts of reductant, and after the cycle, the number of PSII molecules in each particular state, the fraction of centers inactivated, and the fraction Mn bound were stored. Therefore, the number of PSII centers in each particular state, the fraction of centers inactivated, and the fraction of Mn bound was stored for each incremental reductant/PSII ratio. In each simulation, PSII centers were selected to react randomly. Each step in the mechanism was assigned a reaction probability, k_n, as defined above, which was a number between 0 and 1; the reaction step with the greatest probability was always assigned a value of 1. Once a PSII center was selected, a random number between 0 and 1 was assigned to that center. If the random number was less than the probability assigned to the *i*th step, the PSII center would be reduced to the next intermediate in the mechanism; otherwise the center was left undisturbed. For example, the notation $k_1 = 0.1$, $k_2 = 1$, and $k_3 = 0.011$ is used to indicate that the probability of step 2 was 9 times more likely than step 1 and about 90 times more than step 3. For example, in the case of the reaction sequence $S_1 \rightarrow S_{-1} \rightarrow S_{-3} \rightarrow S_{-5}$, a PSII center in S_{-1} is 9 times more likely to undergo a reduction reaction than a center in S_1, and 90 times more likely to react than a center in S_{-3}. If a PSII center was reduced to the next state in the mechanism, it was assumed that the assigned number of reductant molecules had been consumed. Fully reduced centers were excluded from reacting with additional reductant molecules. Mn release simulations were calculated in the same manner as described above, with each PSII center assigned 4 Mn atoms. Release of Mn atoms was imposed after various reduced states had been attained.

Although reasonable simulations could be obtained by assuming different reaction probability parameters for each individual data set under the same conditions, the same assumptions were applied to fit data in all experiments that were carried out under the same conditions in the 24 h incubations. For example, the same reaction probabilities and mechanism were used to model the data in Figures 4B, 5B, and 5D. However, the Mn(II) release and inactivation constraints, but not reaction probabilities, were, at times, varied between experiments that did or did not have additions of 50 mM Ca^{2+} before assay (Figure 4B, open and closed symbols, for example). Models for Mn release were correlated with the models for activity loss; Mn(II) release was allowed to occur only in PSII centers that were assumed to be inactive with respect to O_2 evolution.

After data were collected and plotted, a spline was fit through the simulated data points, using Sigma Plot 2001, to represent a particular simulation fit line. A large number of models were tested, and the inhibition mechanisms that were successfully used to fit the experimental data obtained in the experiments, or otherwise described in Results, are shown below:

Model 1

$$S_1 \xrightarrow[k_1]{1H_2Q} S_{-1}\,(\text{inactive}) \xrightarrow[k_2]{1H_2Q} S_{-3}\,(\text{inactive}) \xrightarrow[k_3]{1H_2Q} S_{-5}\,(\text{inactive})$$

Model 2

$$Y_D^{\bullet}S_1 \xrightarrow[k_1]{NH_2OH} Y_D^{\bullet}S_0 \xrightarrow[k_2]{NH_2OH} Y_D^{\bullet}S_{-1} \xrightarrow[k_3]{NH_2OH} Y_D^{\bullet}S_{-2} \xrightarrow[k_4]{NH_2OH} Y_D^{\bullet}S_{-3} \xrightarrow[k_5]{NH_2OH} Y_D^{\bullet}S_{-4} \xrightarrow[k_6]{NH_2OH} Y_D^{\bullet}S_{-5} \xrightarrow[k_7]{NH_2OH} Y_DS_{-5} \xrightarrow[k_8]{NH_2OH} Y_DS_{-6}$$

(In this mechanism, S_{-3}, S_{-4}, S_{-5}, and S_{-6} are inactive states, and the $S_{-5} \rightarrow S_{-6}$ step refers to reduction of an unidentified oxidant.)

Model 3

$$Y_D^{\bullet}S_1 \xrightarrow[k_1]{2NH_2OH} Y_D^{\bullet}S_{-1} \xrightarrow[k_2]{2NH_2OH}$$

$$Y_D^{\bullet}S_{-3}\ (\text{inactive}) \xrightarrow[k_3]{2NH_2OH}$$

$$Y_D^{\bullet}S_{-5}\ (\text{inactive}) \xrightarrow[k_4]{2NH_2OH} Y_DS_{-5}\ (\text{inactive})$$

Most of the proposed reduced states (S_{-1}, S_{-2}, S_{-3}, S_{-4}, S_{-5}) in the above mechanisms have been either demonstrated or hypothesized to exist (*20*−*22*, *28*−*30*). Because NH_2OH reduces $Y_D^{\bullet}$ (or because $Y_D^{\bullet}$ can be reduced by the Mn cluster in some circumstances (*9*, *28*)), some of the states in models 2 and 3 are unlikely to represent reduced derivatives of only the OEC Mn cluster, and should more appropriately be viewed in terms of the number of NH_2OH molecules consumed by a PSII center (see Discussion). In model 1, H_2Q molecules react with each PSII center individually; a total of 3 H_2Q molecules react with each PSII center in a polypeptide-depleted preparation. Reaction of the first H_2Q molecule inhibits the PSII center, but each PSII center possesses a total of 6 oxidizing equivalents. Model 2 predicts that 8 NH_2OH molecules react with the OEC, but only 4 of these reductant molecules are required to inactivate each PSII center, and it was assumed that each NH_2OH could react individually. Model 3 represents a process where two NH_2-OH react cooperatively with the PSII OEC in two-electron reduction steps. Populations of S_{-1} centers are capable of evolving oxygen, centers reduced to S_{-3} (or further) are inactive, but some centers (S_{-3} and S_{-5}) still contain oxidizing equivalents. In models 2 and 3, reduced intermediates in at least some PSII centers are capable of evolving O_2 upon illumination. This is in contrast with model 1, in which all reduced states were assumed to be inactive. As noted in the reactions, in all cases H_2Q was treated as a two-electron reducing agent, whereas each NH_2OH was modeled as a one-electron reductant, with the exception of the reaction $Y_D^{\bullet}S_{-5} \rightarrow Y_DS_{-5}$, which is discussed in Results.

RESULTS

The extents of inhibition of O_2 evolution and of Mn(II) release caused by H_2Q and NH_2OH reduction of PSII were quantified. For experiments using NH_2OH, intact PSII centers were employed, while salt-washed PSII preparations were exposed to the larger two-electron reductant H_2Q (*30*, *31*, *38*). All incubations were carried out in darkness at 4−8 °C for 24 h to allow for complete reaction between a reductant and the OEC. Figure 1 shows the effects of increasing concentrations of H_2Q on inhibition of O_2 evolution activity in salt-washed PSII centers**.** Inactivation of the OEC appears to attain saturation between 2 and 3 mol of H_2Q/mol of PSII. Figure 1A also shows the best simulated fit to the data points (solid line), which was obtained using the mechanism described by model 1 (see Materials and Methods), where the reaction probabilities are $k_1 = 0.11$, $k_2 = 1$, and $k_3 = 0.011$ and 3 H_2Q molecules react with a PSII center. Figures 1B and 1C show results from similar experiments in which 10 mM Ca^{2+} was added to the salt-washed PSII membranes to replace Ca^{2+} lost during extraction of the extrinsic polypeptides (1B) or where 1 mM EDTA was added to chelate Mn(II) released from the OEC (1C).

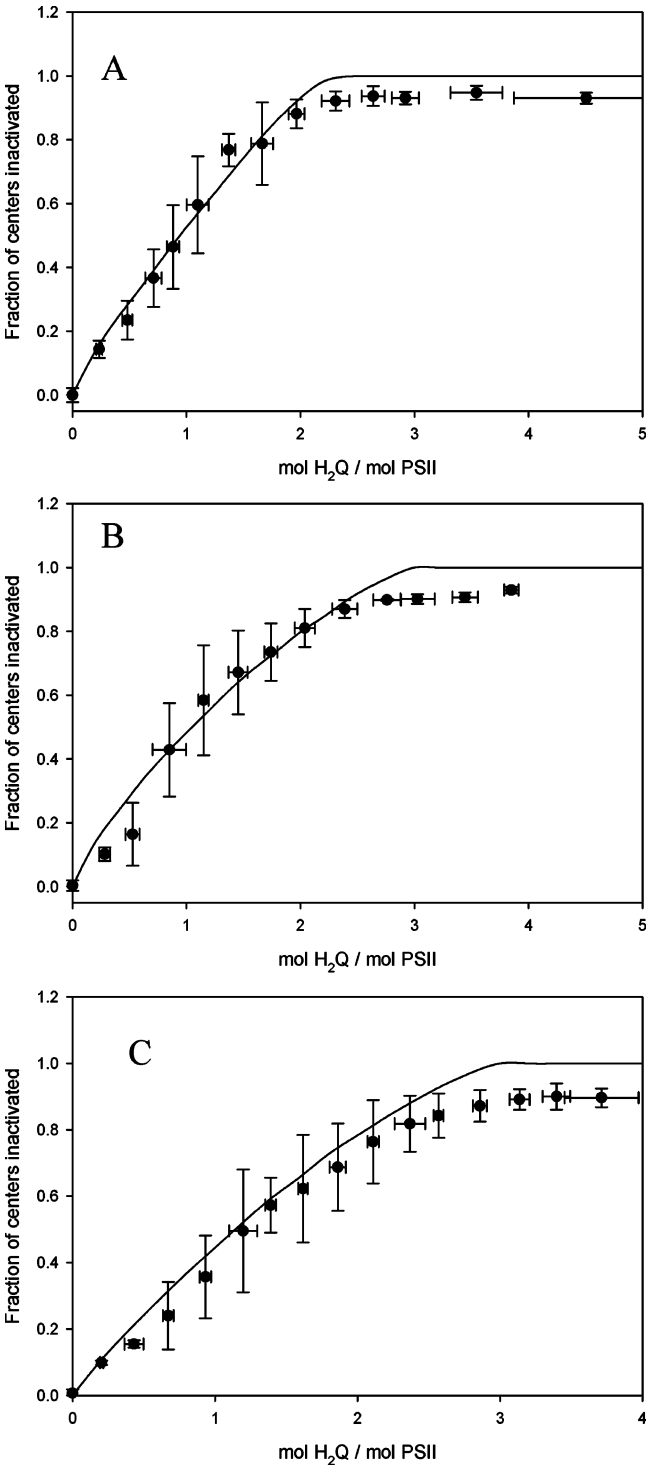

FIGURE 1: Effect of increasing H_2Q/PSII ratios on inhibition of O_2 evolution in SWPSII as a result of a 24 h dark incubation at 4 °C. All samples were assayed for O_2 evolution activity at the end of the incubation period, as described in Materials and Methods. The solid lines in the figures are simulated curves based on model 1 (see Materials and Methods and Table 1 for probability parameters). The following additions were present during the H_2Q incubation period: (A) none, $R^2 = 0.9792$; (B) 10 mM Ca^{2+}, $R^2 = 0.9408$; (C) 1 mM EDTA, $R^2 = 0.9658$.

Model 1 was used to fit these data, using $k_1 = 0.22$, $k_2 = 1$, and $k_3 = 0.11$ (Figure 1B) and $k_1 = 0.011$, $k_2 = 1$, and $k_3 = 0.011$ (Figure 1C). Regardless of the quality of the fits of the data from these experiments to the model ($R^2 > 0.94$), loss of O_2 evolution in all cases saturates at a reductant

Table 1: Summary of the Probability, Mn Release, and Inactivation Parameters Used To Fit H_2Q Data (Figures 1−3)[a]

preparation	50 mM Ca^{2+} added after reductant incubation	reaction probabilities	Mn release	inactive states
SWPSII	−	$k_1 = 0.11$, $k_2 = 1$, $k_3 = 0.011$	1 Mn @ S_{-1} 1 Mn @ S_{-3}	S_{-1}, S_{-3}, S_{-5}
SWPSII + Ca^{2+}	−	$k_1 = 0.22$, $k_2 = 1$, $k_3 = 0.11$	2 Mn @ S_{-1} 1 Mn @ S_{-3}	S_{-1}, S_{-3}, S_{-5}
SWPSII + EDTA	−	$k_1 = 0.011$, $k_2 = 1$, $k_3 = 0.011$	2 Mn @ S_{-1} 1 Mn @ S_{-3}	S_{-1}, S_{-3}, S_{-5}
SWPSII	+	$k_1 = 0.11$, $k_2 = 1$, $k_3 = 0.011$	2 Mn @ S_{-1} 1 Mn @ S_{-3}	S_{-1}, S_{-3}, S_{-5}
SWPSII + Ca^{2+}	+	$k_1 = 0.22$, $k_2 = 1$, $k_3 = 0.11$	2 Mn @ S_{-1} 1 Mn @ S_{-3}	S_{-1}, S_{-3}, S_{-5}
SWPSII + EDTA	+	$k_1 = 0.011$, $k_2 = 1$, $k_3 = 0.011$	2 Mn @ S_{-1} 1 Mn @ S_{-3}	S_{-1}, S_{-3}, S_{-5}

[a] Reaction 1, $S_1 \xrightarrow{k_1} S_{-1} \xrightarrow{k_2} S_{-3} \xrightarrow{k_3} S_{-5}$ was used to fit the data in all cases. When present during the reductant incubation step, the Ca^{2+} concentration was 10 mM, and that of EDTA was 1 mM

concentration in excess of 2 mol of H_2Q/mol of PSII, a finding that suggests that each center reacts with more than 2 mol of the 2-electron reductant. This is most apparent in the case of PSII centers incubated with reductant and 1 mM EDTA; in the presence of the chelator, activity inhibition clearly attained saturation at 3 mol of added reductant. The results of all of these experiments are summarized in Table 1.

In a second set of reduction titrations with H_2Q, 50 mM $CaCl_2$ was added to each sample after the 24 h incubation period to displace any loosely bound Mn(II) generated by the reductant. After incubation periods of 30−60 min, the samples were assayed, and no additional losses of activity were observed (data not shown). Because extraction of any loosely bound Mn(II) by Ca^{2+} does not affect the residual activity of these samples, this population of Mn(II) must be associated with inhibited centers that are incapable of undergoing photoactivation. Therefore, the products of reduction of the Mn cluster must be unstable under the long-term incubation conditions used here.

In addition to characterizing the relationship between loss of O_2 evolution activity and H_2Q concentration, Mn(II) release from salt-washed PSII was also quantified in order to gain insight into the mechanism of H_2Q reduction of OEC Mn. Salt-washed PSII samples were incubated for 24 h in darkness in the presence of increasing concentrations of H_2Q, after which 50 mM $CaCl_2$ was added to displace any adventitiously bound Mn(II). The samples were centrifuged, the pellets were acidified in 0.6 M HCl, and the Mn(II) contents of the pellets were determined by EPR, as described in Materials and Methods. Control samples that were incubated for 24 h in darkness and subjected to the same treatment were found to retain 90% of bound Mn relative to freshly thawed samples (data not shown).

Regardless of the treatment applied to the salt-washed PSII membranes, Mn release appeared to saturate at more than 2 mol of H_2Q/mol of PSII (Figure 2), and markedly so in the sample reduced in the presence of 1 mM EDTA (Figure 2C). For these samples, Mn release reached a maximum value at about 3 H_2Q/PSII. Model 1 was used to fit the data in all three cases, although the assumptions needed to fit the Mn release data differed for the various experimental conditions. These are summarized in Table 1; identical reaction probabilities were used to fit the data from all experiments conducted under the same conditions (Figures 1 and 2). An interesting outcome of the Mn(II) quantification experiments is the finding that approximately 25% of the Mn remained bound in all cases, corresponding to retention by PSII of about 1 Mn per reaction center. Although this might, in theory, be a redox inert Mn, the simulations used to model Mn reduction in these samples indicate that it is more likely that this remaining Mn is reduced by H_2Q, but remains tightly bound at a site where it is not easily displaced by addition of 50 mM Ca^{2+}. This is consistent with the goodness of fit ($R^2 > 0.92$) for the simulations of the Mn release data that assume that PSII centers react with 3 H_2Q molecules. If either 10 mM Ca^{2+} or 1 mM EDTA was present during reduction of samples with H_2Q, then no additional loss of Mn(II) was observed upon addition of 50 mM Ca^{2+} prior to the centrifugation and acidification steps. In contrast, salt-washed PSII centers incubated in the absence of either Ca^{2+} or EDTA during H_2Q reduction retain approximately 50% of the Mn-(II), or 2 Mn(II)/PSII, if 50 mM Ca^{2+} is not added to displace adventitiously bound Mn(II) prior to centrifugation and acidification of the resulting pellet (Figure 3). A similar sample incubated in the presence of 4 equiv of H_2Q for 24 h and then washed with SMN retains 25−35% of the Mn (data not shown), indicating that one of the two residual Mn atoms is adventitiously bound. The data in Figure 3 were fit ($R^2 = 0.8166$) using the mechanism in model 1 and the same probability parameters that were used in Figures 1A and 2A. Clearly, these samples retained higher amounts of Mn than can be accounted for by this model. A likely explanation for the discrepancy is that the samples were not treated with 50 mM Ca^{2+} to displace heterogeneously bound Mn(II), which might account for the nonstoichiometric Mn release observed. A significantly improved fit ($R^2 = 0.9141$) was achieved for the data in Figure 3 by assuming noninteger release of Mn (1 Mn @ S_{-1}, 0.75 Mn @ S_{-3}, data not shown). The simulations imply that salt-washed PSII centers that are reduced to the S_{-1} state by H_2Q are unstable over 24 h, lose Mn, and are incapable of evolving O_2. Results of these experiments would imply that individual PSII centers react with three H_2Q molecules and, because H_2Q is a two-electron reductant, this stoichiometry suggests that each OEC contains six oxidizing equivalents that react with H_2Q.

The S_1 oxidation states of OEC Mn in intact PSII samples were probed using NH_2OH. Because these preparations contain the full complement of extrinsic polypeptides and Ca^{2+}, no experiments were conducted in which the metal

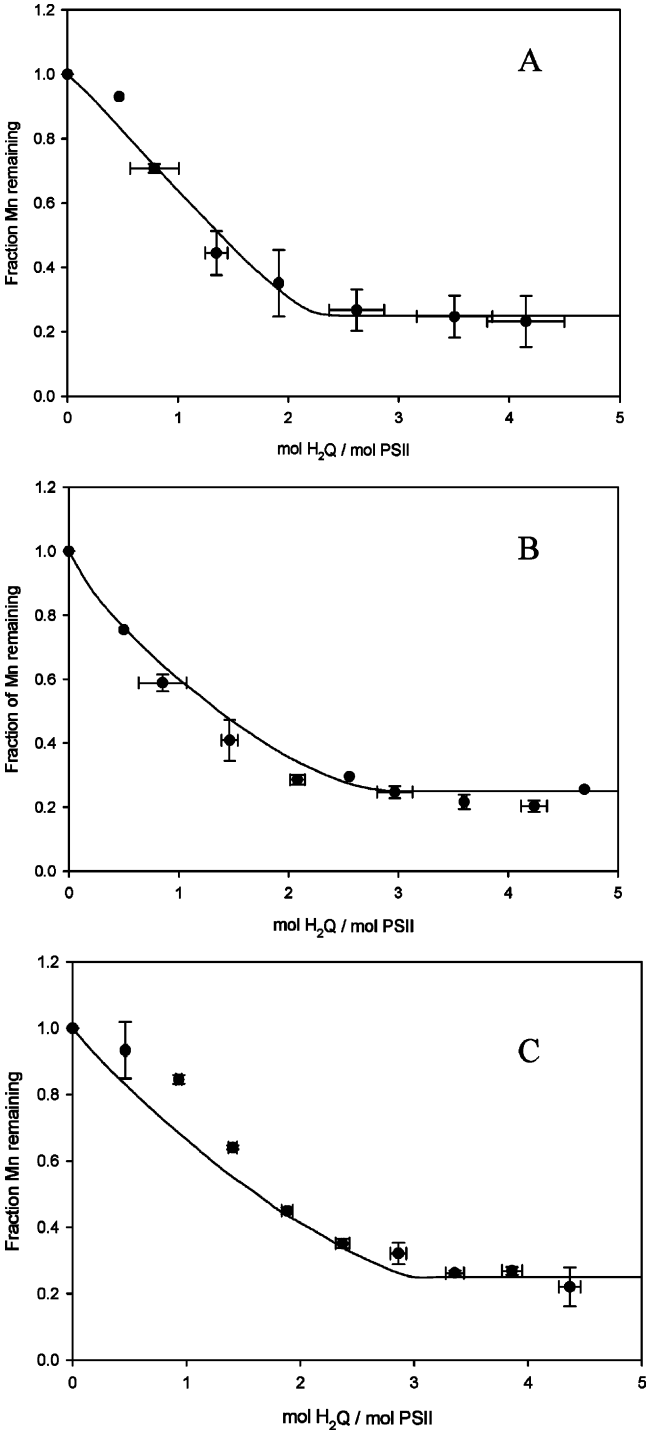

FIGURE 2: Effect of increasing H_2Q/PSII ratios on Mn(II) release from acidified SWPSII following a 24 h dark incubation with H_2Q. At the end of the incubation period, 50 mM Ca^{2+} was added to the samples to release adventitiously bound Mn(II) prior to centrifugation and acidification of the resulting pellet. The solid line is a simulation based on model 1, and probability parameters are given in Table 1. The additions during H_2Q incubation were as follows: (A) none, $R^2 = 0.9701$; (B) 10 mM Ca^{2+}, $R^2 = 0.9618$; (C) 1 mM EDTA, $R^2 = 0.9283$.

was added during reductant incubations. The representative data shown in Figure 4A illustrate the results that were obtained without addition of EDTA during the 24 h reductant incubation. The solid line is a simulation based on model 3 that assumes that centers reduced to S_{-3} are inactive, and that $k_1 = 1$, $k_2 = 1$, $k_3 = 1$, and $k_4 = 0.11$ ($R^2 = 0.9558$). In

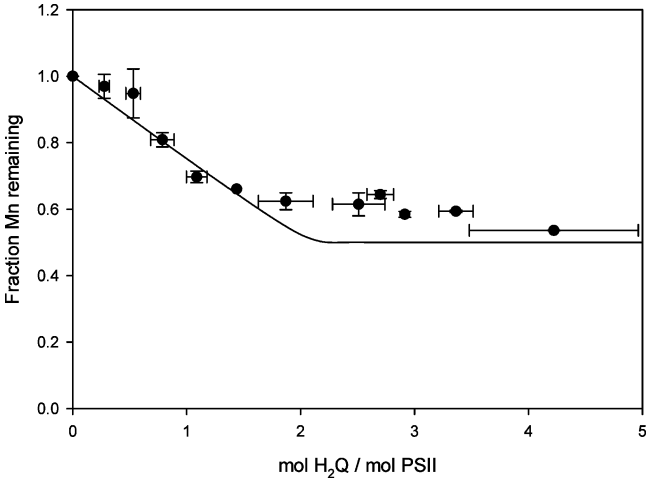

FIGURE 3: Failure to add 50 mM Ca^{2+} to H_2Q-reduced PSII increases retention of Mn(II). SWPSII samples were incubated with no additions, and the samples were centrifuged and acidified without further treatment. The solid line is a simulation using model 1. The Mn release parameters are given in Table 1, $R^2 = 0.8166$.

Figure 4B, the closed symbols show the results for samples incubated with NH_2OH in the presence of 1 mM EDTA. The solid line is a simulation based on model 3 with inactive S_{-3} centers that assumes that $k_1 = 0.33$, $k_2 = 1$, $k_3 = 0.33$, and $k_4 = 0.33$ ($R^2 = 0.9928$). The effect of exposing these samples to 50 mM Ca^{2+} after NH_2OH reduction is indicated by the open symbols, and the dashed line is a simulation, using model 3, that assumes that S_{-1} centers are inactive ($R^2 = 0.9870$). If 50 mM Ca^{2+} is omitted prior to assay (Figures 4A and 4B, closed circles), inactivation of the OEC attains saturation at approximately 8 mol of reductant/mol of PSII. This would indicate that PSII contains 8 oxidizing equivalents that can react with NH_2OH, assuming that it acts as a 1-electron reductant. Samples reduced in the presence of EDTA and then exposed to 50 mM Ca^{2+} prior to assay showed a nearly complete loss of O_2 evolving activity at between 5 and 6 mol of NH_2OH/PSII (Figure 4B, open symbols), a lower reductant/PSII ratio than is obtained when Ca^{2+} addition is omitted after equilibration of the sample with NH_2OH (Figure 4B, closed symbols). The best simulation of these data is given by model 3 with $k_1 = 0.33$, $k_2 = 1$, $k_3 = 0.33$, and $k_4 = 0.33$, in which states reduced to S_{-1} (or lower) were assumed to be inactive. Thus, in the presence of EDTA, addition of 50 mM Ca^{2+} just prior to activity assays causes a shift in the loss of O_2 evolution activity to lower NH_2OH concentrations, in contrast to what was observed with H_2Q treated SWPSII. In either the absence or presence of EDTA, a good fit to the data is obtained with model 3 (Figures 4A and 4B, solid lines) using the reaction probabilities shown in Table 2. The simulations of these experiments indicated that intact PSII samples in S_{-1}, if they were not further perturbed, were capable of evolving O_2, in contrast to the studies done with salt-washed centers treated with H_2Q.

Figure 5A presents the results of quantifications of Mn release from the OEC after exposure to NH_2OH, carried out without additions of Ca^{2+} or EDTA to remove adventitious Mn(II). The results are in good agreement with the O_2 evolution data; model 3, with appropriate parameters, was used to fit the data ($R^2 = 0.9319$). As can be seen, Mn release reached a maximum at 8 mol of NH_2OH where about 50%

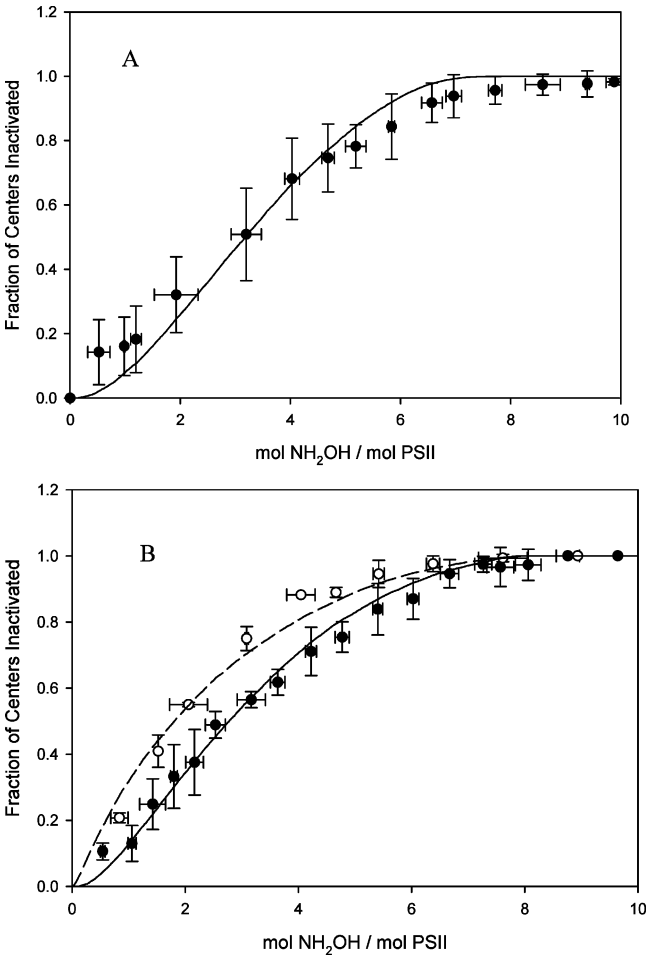

FIGURE 4: Effect of increasing NH_2OH/PSII ratios on inhibition of O_2 evolution activity. Samples were incubated for 24 h in darkness. At the end of the incubation period, O_2 evolution was assayed in 10 mM $CaCl_2$ and 50 mM MES (pH 6.0) as described in Materials and Methods. (A) Samples incubated with no additions, $R^2 = 0.9558$. The solid line is a simulation based on model 3 and assumes that centers in S_{-3} are inactive. The probability parameters are given in Table 2. (B) Samples incubated with NH_2OH and 1 mM EDTA. At the end of the incubation period samples were assayed for activity immediately (closed symbols) or after exposure to 50 mM Ca^{2+} (open symbols). The simulations are as follows: solid line, model 3, assuming that S_{-3} is inactive (see Materials and Methods and Table 2 for probability parameters), $R^2 = 0.9928$; dashed line, model 3 with the same parameters and assuming that S_{-1} is inactive, $R^2 = 0.9870$.

of the Mn was extracted from the OEC. At least some of the remaining Mn(II) in this sample is weakly bound. An experiment in which intact PSII samples were incubated with 10 equiv of NH_2OH and then washed with SMN lost additional Mn (data not shown). Incubation of intact PSII samples with NH_2OH and 1 mM EDTA caused a nearly complete release of Mn (Figure 5B). In this case, model 3 (using the same parameters as were used for the O_2 evolution data, see Table 2) again gave the best fit of the data in Figure 5B (solid line, $R^2 = 0.9770$); 3 Mn(II) were assumed to be released from S_{-3}, and 1 Mn(II) was assumed to be released from Y_DS_{-5}.

Release of Mn(II) occurred at lower molar ratios of NH_2-OH when 50 mM Ca^{2+} was added to samples after long-term reductant incubation (Figures 5C and 5D). The best model to explain these results used a simulation based on model 3 ($R^2 = 0.9689$ for the fit of data in Figure 5C, $R^2 = 0.9271$ for the fit of data in Figure 5D). In this case, it was necessary to assume that Mn(II) is released from centers reduced to S_{-1}, or to lower S states. Because Ca^{2+} would displace any loosely bound Mn(II), it is likely that active reduced states (S_{-1} in model 3, for example) are metastable; that is, they can evolve O_2 upon illumination but are inhibited by Mn(II) release upon addition of Ca^{2+} in the dark. This hypothesis is consistent with the data shown in Figure 4B (open symbols, dashed line), where Ca^{2+} addition after reductant incubation shifts activity loss to lower NH_2OH/PSII ratios. A summary of these experiments and simulations may be found in Table 2.

The fit to the data in Figure 5D is unsatisfactory in the region of 3−5 mol of NH_2OH/PSII. A less marked deviation can be seen in the same NH_2OH concentration range of the O_2 evolution data of Figure 4B (open symbols). In these experiments, the actual Mn(II) and activity losses exceeded what was reasonably predicted by any of the models tested. Because high ionic strength coupled with NH_2OH reduction has been shown to remove the 17 kDa and 23 kDa polypeptides and to destabilize MSP binding (*39*), a salt-washed PSII preparation was exposed to NH_2OH under the same conditions as in Figure 5D and assayed for O_2 evolution activity and Mn content. Activity inhibition and Mn(II) release saturated at 2−3 mol of NH_2OH/mol of PSII in these samples (data not shown). Therefore, the additional loss of Mn observed in intact PSII preparations may be due to NH_2-OH-induced release of the extrinsic polypeptides and, therefore, to loss of additional Mn when EDTA is present.

Because maximum Mn(II) release and inhibition of O_2 evolution activity appear to occur in most cases at 8 mol of NH_2OH (without Ca^{2+} addition) in intact PSII preparations, attempts were made to identify other possible oxidants that might react with NH_2OH. Intact PSII membranes were incubated in the presence of NH_2OH for 24 h at 4 °C in darkness, and the EPR spectrum of the dark stable $Y_D^{\bullet}$ species was monitored. As shown in Figure 6, the $Y_D^{\bullet}$ signal was diminished in intensity by NH_2OH, as compared to control samples; loss of signal saturates at ∼8 mol of NH_2-OH/mol of PSII (Figure 6, closed symbols). In addition, significant reduction of the $Y_D^{\bullet}$ signal occurs at low NH_2-OH concentrations, which may indicate that this reaction occurs on the same time scale as the reaction between NH_2-OH and OEC Mn. Therefore, $Y_D^{\bullet}$ is clearly a source of additional oxidizing equivalents in PSII under the incubation conditions used in these experiments. When H_2Q was tested in similar experiments, a diminished loss of $Y_D^{\bullet}$ intensity was observed (Figure 6, open symbols), relative to the result with NH_2OH. If $Y_D^{\bullet}$ supplies a single oxidizing equivalent per PSII center during the reaction with NH_2OH, then the stoichiometries shown in Figures 4 and 5 could be explained by one of the following conditions:

(1) $Y_D^{\bullet}$ and an unassigned species supply two electron equivalents to the OEC.

(2) $Y_D^{\bullet}$ supplies a single oxidizing equivalent to the OEC in a reaction requiring 2 NH_2OH.

Cytochrome b559 is also a potential oxidant in these experiments, and this introduces a complication that cannot be controlled. Salt washing and/or Mn loss from PSII shifts the potential of b559 from high potential to low potential, and in this form the cytochrome is oxidized (*40*, *41*). Low-potential b559 is not reduced by H_2Q (*42*) or by NH_2OH

Table 2: Summary of Probability, Mn Release, and Inactivation Parameters Used To Fit NH_2OH Data (Figures 4 and 5)[a]

preparation	50 mM Ca^{2+} added after reductant incubation	reaction probabilities	Mn release	inactive states
intact	−	$k_1 = 1, k_2 = 1,$ $k_3 = 1, k_4 = 0.11$	2 Mn @ S_{-3}	S_{-3}, S_{-5}, Y_DS_{-5}
intact + EDTA	−	$k_1 = 0.33, k_2 = 1$ $k_3 = 0.33, k_4 = 0.33$	3 Mn @ S_{-3} 1 Mn @ Y_DS_{-5}	S_{-3}, S_{-5}, Y_DS_{-5}
intact	+	$k_1 = 1, k_2 = 1,$ $k_3 = 1, k_4 = 0.11$	3 Mn @ S_{-3}	S_{-3}, S_{-5}, Y_DS_{-5}
intact + EDTA	+	$k_1 = 0.33, k_2 = 1$ $k_3 = 0.33, k_4 = 0.33$	1 Mn @ S_{-1} 2 Mn @ S_{-3} 1 Mn @ S_{-5}	S_{-1}, S_{-3}, S_{-5}, Y_DS_{-5}

[a] Reaction 3, $Y_D^{\bullet}S_1 \xrightarrow{k_1} Y_D^{\bullet}S_{-1} \xrightarrow{k_2} Y_D^{\bullet}S_{-3} \xrightarrow{k_3} Y_D^{\bullet}S_{-5} \xrightarrow{k_4} Y_DS_{-5}$ (see Materials and Methods and figure legends) was used to fit the data. When it was present during the reductant incubation step, the EDTA concentration was 1 mM.

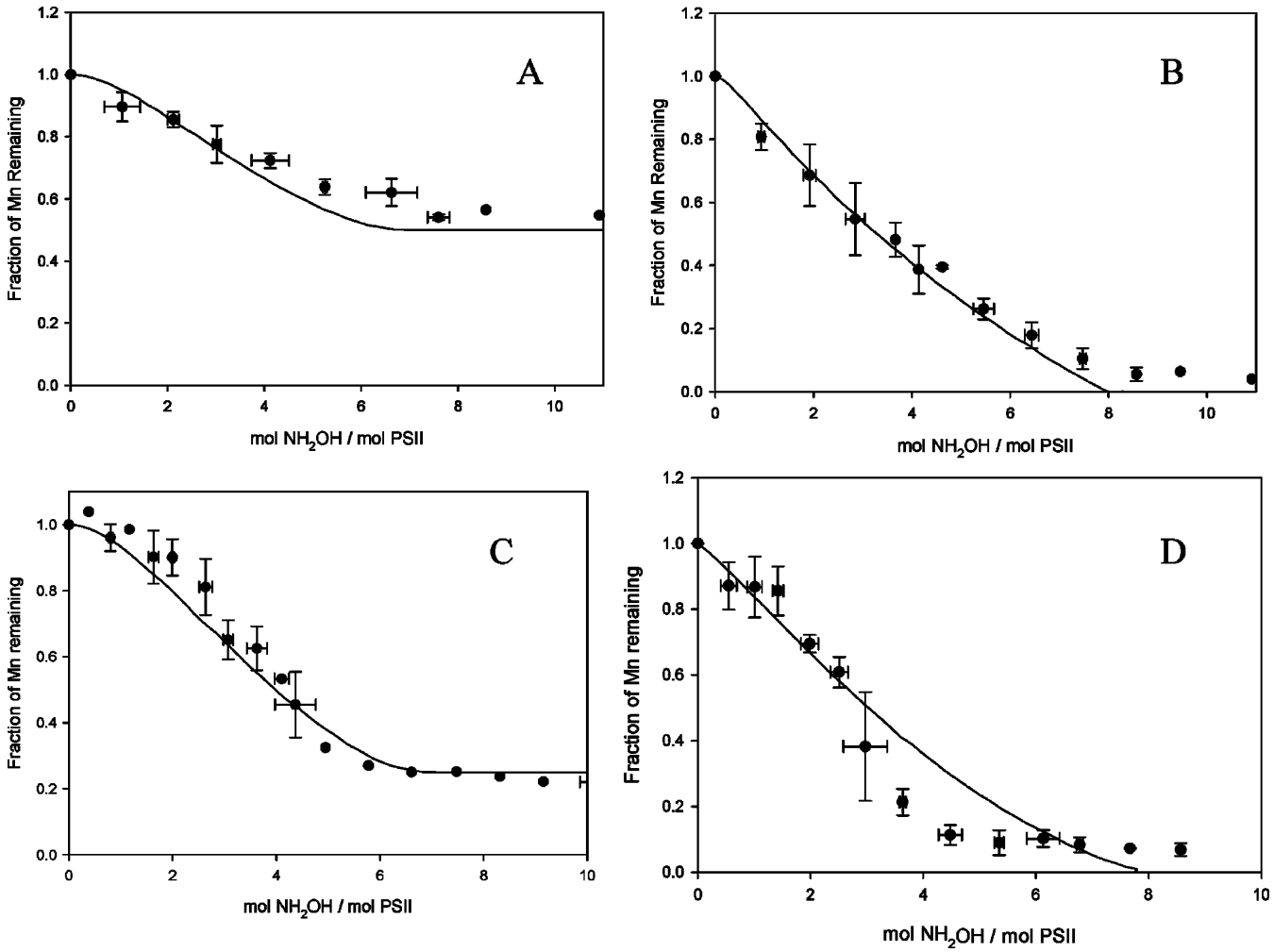

FIGURE 5: (A) Mn(II) release from acidified intact PSII samples incubated with NH_2OH for 24 h. The solid line is a simulation based on model 3 (see Materials and Methods), $R^2 = 0.9319$. (B) Data from incubation experiments carried out in the presence of 1 mM EDTA. The solid line is a simulation based on model 3. Probability and Mn release parameters are given in Table 2, $R^2 = 0.9770$. (C) Same as panel A, but 50 mM Ca^{2+} was added to the samples before centrifugation and acidification of the resulting pellet. The solid line is a simulation based on model 3; see Table 2, $R^2 = 0.9689$. (D) Same as panel B, but 50 mM Ca^{2+} was added to the samples before centrifugation and acidification of the resulting pellet. The solid line is a simulation based on model 3. Probability and Mn release parameters are given in Table 2, $R^2 = 0.9271$.

(data not shown), and is therefore unlikely to be a source of the additional NH_2OH reducing equivalents consumed in reduction of the OEC.

DISCUSSION

Spectroscopic techniques (CW and pulsed EPR, XANES spectroscopy) (*11*, *15*, *16*, *27*, *43*, *44*) have been the principal source of data used to estimate the oxidation states of Mn atoms in the S_1 state. These methods utilize the properties of synthetic Mn compounds of known structure and oxidation state as a basis of comparison with spectroscopic properties of the OEC in order to generate models of the PSII Mn cluster. XANES results are consistent with models in which the S_1 Mn oxidation states are 2 Mn(III) and 2 Mn(IV) (*10*,

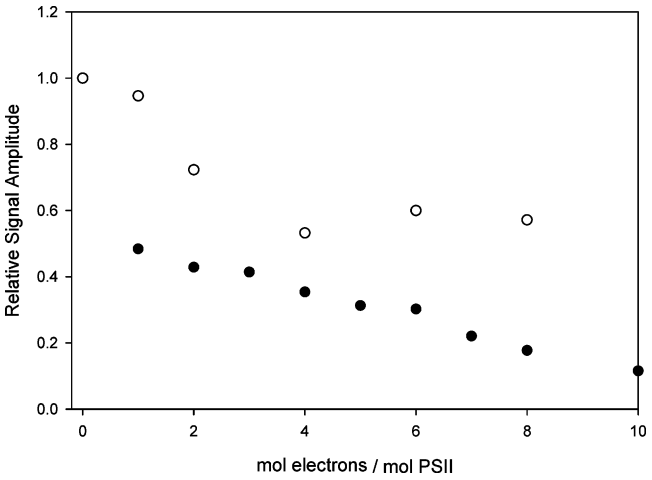

FIGURE 6: Effect of 24 h dark incubations with NH_2OH (closed symbols, intact PSII) or H_2Q (open symbols, SWPSII) on the $Y_D^•$ EPR signal amplitude. After 24 h, 1 mM EDTA was added to the samples to suppress the EPR six-line Mn(II) signal. The signal amplitude for a control (intact) PSII sample incubated under the same conditions as the NH_2OH sample was 75% of the amplitude after the sample was illuminated for 1 min under room light. The control SW PSII sample for H_2Q experiments, incubated for 24 h in darkness, had a signal amplitude that was 60% of the same sample after 1 min of illumination under room light. The electron stoichiometry was calculated assuming 1 electron per NH_2OH and 2 electrons per H_2Q. Spectrometer conditions are given in Materials and Methods.

11). In the case of EPR, there was early agreement that the S_2 multiline signal could be approximated by a similar signal associated with a di-μ-oxo bridged Mn(III)−Mn(IV) dimer (*45*−*47*). However, the failure of synthetic mixed valence binuclear Mn clusters possessing these oxidation states to produce exact matches to the S_2 EPR multiline signal and the observation of a modification by NH_3 of the $g = 4.1$ form of the S_2 EPR signal (appearance of hyperfine structure) have provided strong support for the proposal that couplings among all four Mn atoms of the OEC are required to produce satisfactory simulations of the $g = 2$ multiline signal (*48*, *49*). Although results from pulsed EPR and XANES experiments are interpreted as supporting Mn oxidation states of $Mn(III)Mn(IV)_3$ in S_2 (*15*, *16*, *43*), attempts to simulate the S_2 multiline signal have also succeeded using Mn oxidation states of $Mn(III)_3Mn(IV)$(*14*).

The experiments reported here are the first to obtain the reductant stoichiometries for O_2 evolution inhibition and Mn(II) release, and to use these results to estimate Mn oxidation states in S_1. In the case of both H_2Q and NH_2OH, and in two different preparations, at least six electrons per PSII reaction center appear to be necessary to inactivate the OEC and to produce maximum release of Mn(II) from the OEC. Control experiments to test the stability of the reductants indicate that, under the experimental conditions used here, NH_2OH and H_2Q are both resistant to autoxidation, or to reactions with other components (buffers, salts, sucrose) of the solvent system used to suspend PSII. In addition, experiments that included EDTA to chelate Mn(II), or trace metal contaminants that might oxidize the reductants, produced little effect on the overall stoichiometries of NH_2OH and H_2Q consumption in these long-term incubations (Figures 2, 4, and 5). Therefore, the primary cause of reductant oxidation in these experiments is due predominantly to reduction of the OEC Mn cluster.

In the case of H_2Q, the best fits of the data on both Mn(II) release and inhibition of O_2 evolution activity were consistently obtained by assuming that SWPSII centers react with 3 H_2Q molecules (model 1 in Materials and Methods, with appropriate probability modifications given in Table 1). Addition of 50 mM Ca^{2+} to remove adventitiously bound Mn(II) following a long-term incubation step, but prior to assay, had no effect on activity inhibition, which suggests that Mn(II) is released from H_2Q incubated SWPSII samples under conditions where the OEC is not completely reduced. Hydroquinone has been shown to reduce Mn model compounds by two electron reduction mechanisms (*50*, *51*), in agreement with EPR and XANES results showing that H_2Q reduces PSII centers preincubated with Ca^{2+} by two electrons (*11*, *30*), to yield a stable $Mn(II)_2Mn(IV)_2$ cluster. If each H_2Q reduces the OEC Mn by 2 equiv, then the stoichiometries of inhibition of O_2 evolution and of Mn release indicate that the Mn cluster in S_1 contains more than 4 oxidizing equivalents. This is consistent with best fits of the data from all titrations using H_2Q, which require that the OEC Mn cluster contains a total of 6 oxidizing equivalents. A reaction between H_2Q and $Y_D^•$ was not accounted for in fitting the data because oxidation of H_2Q by other components of PSII does not appear to be a significant factor in these experiments; the reaction of H_2Q with $Y_D^•$ occurs in at most 25% of PSII centers in 24 h at 3−4 mol of H_2Q/mol of PSII, when the dark decay of $Y_D^•$ in control SWPSII over the same time period is accounted for (Figure 6). Thus, H_2Q reacts predominantly with the PSII Mn cluster, and the data from this reaction provide chemical evidence that the oxidation state of the OEC Mn cluster in the S_1 state is most likely $Mn(III)_2Mn(IV)_2$.

The reaction probabilities needed to fit the data from the H_2Q experiments provide some insight into the structure and reactivity of the OEC Mn cluster. Under any of the experimental conditions used here, the $S_{-1} \rightarrow S_{-3}$ step (modeled with k_2) would fit the data only if it was assigned the highest reactivity in the mechanism (model 1). In most cases, the $S_{-3} \rightarrow S_{-5}$ step (modeled with k_3) was required to be the least reactive step, and the $S_1 \rightarrow S_{-1}$ step (modeled with k_1) was usually between these two extremes. This suggests that S_{-1} is more reactive toward H_2Q reduction than either S_1 or S_{-3} and, surprisingly, that S_{-3} is quite stable with respect to reduction by H_2Q. This, in conjunction with the modeling of Mn release that predicts a loss of 3 Mn in S_{-3} in all cases (Table 1), could indicate that S_{-3} contains a single Mn(IV) that reacts slowly with H_2Q. Alternatively, the stability of S_{-3} predicted by these fits could reflect the presence of a kinetic impediment; for example, steric factors may prevent facile access of H_2Q molecules to one of the Mn atoms of the cluster. If the reaction probabilities used to model the data accurately reflect the mechanism of OEC Mn reduction, it seems unlikely that the high population of S_{-1} PSII centers that were previously detected could have been observed (*30*). However, those experiments were carried out in the presence of Ca^{2+} under conditions (short (30 min) incubation time, 20 mol of H_2Q/mol of PSII) that are very different from the 24 h incubation periods used here.

The best fits of Mn(II) release and loss of O_2 evolution caused by reduction of the intact OEC with NH_2OH,

when 50 mM Ca^{2+} was not added to displace adventitious Mn(II), were obtained by assuming that 8 NH_2OH react with the OEC. Model 3 in Material and Methods, with modifications presented in Table 2, yields the best fit of the experimental data. The reaction of NH_2OH with $Y_D^{\bullet}$ was included in the model mechanism because this reaction occurs in at least 70% of PSII centers during 24 h incubations at NH_2OH/PSII ratios greater than 6 (Figure 6). If $Y_D^{\bullet}$ reduction is included, the overall stoichiometry is composed of 6 oxidizing equivalents associated with the Mn cluster, 1 oxidizing equivalent from $Y_D^{\bullet}$, and about 1 equivalent from an unknown oxidant. Thus, the activity inhibitions observed with NH_2OH as the reductant are also consistent with a $Mn(III)_2Mn(IV)_2$ cluster in S_1.

The mechanism of reduction of the PSII Mn cluster in two-electron steps, proposed in model 3, although consistent with the results in refs *20*−*25*, does appear to contradict results that showed that both one and two flash delays in O_2 release occur in NH_2OH treated intact thylakoid membranes (*52*, *53*). However, a number of important differences exist between these studies and those reported here. The present experiments were conducted entirely on isolated PSII membranes, in darkness, under incubation conditions (24 h) that allowed for complete reaction of NH_2OH with the OEC. On the other hand, thylakoids that were incubated for short periods (<20 min) with NH_2OH and subsequently flashed yielded one-electron reduced states, some of which were transient in nature (*52*). Because one-electron reduced intermediates can form, model 2, rather than model 3, might better represent the mechanism of NH_2OH induced reduction of the PSII OEC. In fact, model 2 can be used to simulate the data of Figures 4 and 5 (data not shown). These simulations consistently required pairs of 1 electron steps in the mechanism with alternating low and high reaction probabilities, rather than single 2-electron steps as in model 3 (for example, $k_1 = 0.03$, $k_2 = 0.33$, $k_3 = 0.1$, $k_4 = 1$, $k_5 = 0.033$, $k_6 = 0.33$, $k_7 = 0.033$, $k_8 = 0.33$ and S_{-3} inactive for Figure 4B, closed symbols; $k_1 = 0.1$, $k_2 = 1$, $k_3 = 0.1$, $k_4 = 1$, $k_5 = 0.1$, $k_6 = 0.1$, $k_7 = 0.1$, $k_8 = 1$ and S_{-3} inactive for Figure 5B, closed symbols). Inspection of model 2 using these parameters reveals that odd-electron reduced populations in model 2 would be very low. Furthermore, the reduction of $Y_D^{\bullet}$ observed to occur at low molar ratios of NH_2OH/PSII may be caused by $Y_D^{\bullet}$ oxidation of the Mn cluster. Therefore, the presence of intermediate, one-electron reduced states previously observed in flash experiments may be a function of reoxidation of the Mn cluster by $Y_D^{\bullet}$ after NH_2OH exposure, or may be due to oxidation of NH_2OH rather than Mn by $Y_Z^{\bullet}$. Because of these uncertainties, data were analyzed using model 3 rather than model 2 for simplicity of presentation, and because the simulations of model 2 lead to the same conclusions. Consequently, the simulations of inhibition and Mn(II) release data support a mechanism for NH_2OH inactivation of the OEC that creates high populations of centers in S_{-1} and that is consistent with earlier proposals (*20*−*25*). Although NH_2OH is a one-electron reducing agent, it is difficult to envision reactions in which it is oxidized by 1 electron. Several NH_2OH oxidation reactions are shown below (*54*):

(I) $2NH_2OH \rightarrow N_2 + 2H_2O + 2H^+ + 2e^-$

$1e^-$ per NH_2OH

(II) $2NH_2OH \rightarrow N_2O + H_2O + 4H^+ + 4e^-$

$2e^-$ per NH_2OH

(III) $NH_2OH \rightarrow NO + 3H^+ + 3e^-$

$3e^-$ per NH_2OH

(IV) $2NH_2OH \rightarrow NO^{\bullet} + NH_3 + H_2O + H^+ + e^-$

$0.5e^-$ per NH_2OH,

or $1e^-$ per NH_2OH

if $NO^{\bullet}$ is a donor

None of these reactions can provide a satisfactory explanation for the reduction of S_1 to S_0 (*26*, *27*); it is possible that a single NH_2OH could bind to an Mn and undergo oxidation and deprotonation to form an intermediate $Mn^{reduced}$—$^{\bullet}ONH_2$ species. However, if two $NH_2O^{\bullet}$ are bound to adjacent Mn in the same PSII OEC, N_2 and 2 H_2O would probably be released in a reaction equivalent to reactions I. Either reaction IV above or a trapped $Mn^{reduced}$—$^{\bullet}ONH_2$ intermediate could account for the S_0 multiline signal in PSII samples treated with NH_2OH, whereas oxidation mechanism I is much more likely in long-term incubations and occurs in a large percentage of centers according to the simulations reported here.

Since a number of experiments have shown that NH_2OH at low concentrations can form an S_{-1} state (*20*−*25*, *52*, *53*), it is possible that other reactions (II, for example) might be involved in the formation of this state; reaction II has, in fact, been implicated in the reaction between NH_2OH and a binuclear Mn(IV) model compound (*55*). However, if reaction II were the sole mechanism for reduction of S_1 OEC Mn, then the Mn cluster would have to contain a total of 12 to 16 oxidizing equivalents to account for the number of NH_2OH required to inactivate the OEC and produce release of Mn(II), which exceeds the stoichiometries that are obtained from H_2Q titrations or that are predicted by any existing models for the oxidation state of the Mn cluster.

The reaction probabilities used to fit data from the NH_2OH experiments (Table 2) also suggest the presence of a slower reaction in highly reduced S states. Because NH_2OH is much smaller than H_2Q, steric factors should have less of an effect on access of NH_2OH to a Mn(III) or Mn(IV), and this is reflected in the relative probability parameters ($k_2 = 1$, $k_4 = 0.33-0.1$ for NH_2OH; $k_2 = 1$, $k_3 = 0.1-0.011$ for H_2Q). The probability parameters used to fit the data collected in the presence of EDTA suggest that the $S_{-1} \rightarrow S_{-3}$ transition is somewhat faster than the other steps, which is a further indication that S_{-1} is more reactive to reduction by NH_2OH than are the other S states. When combined with the parameters used to fit the H_2Q data, these results support a model for OEC Mn in which 3 atoms of the metal are readily accessed and reduced to form an S_{-3} state, but facile reduction of the remaining Mn is slow, perhaps because of steric factors.

The results of these reductive titrations of the OEC are consistent with reversible inhibition of O_2 evolution in the intact OEC at low reductant concentrations, and irreversible activity inhibition at high concentrations. Inhibition is complete and irreversible if the molar ratio of NH_2OH/PSII is sufficiently high (>8:1) to reduce all OEC Mn to Mn(II), and $Y_D^•$ to Y_D. At low concentrations and short incubation times, reduction of the OEC Mn to 4 Mn(II) would proceed slowly, allowing the formation of the intermediate, metastable reduced states that can be oxidized by exposure of PSII to illumination (*20*−*25*). At high NH_2OH concentrations, the reduction of each cluster would be more rapid, causing a concurrent loss of Mn(II) and O_2 evolution activity by the enzyme. Because $Y_D^•$ participates in the reactions between NH_2OH and PSII, the models proposed for reduction of the OEC do not represent the actual populations of reduced Mn in the samples; for example, the third reductive event in model 1 may represent reduction of $Y_D^•$ and not reduction of the Mn cluster. Furthermore, $Y_D^•$ may oxidize the partially reduced Mn cluster (especially on the time scale of a 24 h incubation) so it is more appropriate to view the simulations in the context of NH_2OH molecules, rather than electrons, consumed by a PSII center. In the case of H_2Q, on the other hand, the simulations probably represent the actual reduced Mn atoms present in these samples.

In contrast to the H_2Q data, only NH_2OH-treated PSII centers incubated with 1 mM EDTA and subjected to addition of 50 mM Ca^{2+} after the 24 h dark incubation could be adequately modeled if it was assumed that Mn release (Figure 5D) and activity inhibition (Figure 4B, open symbols) occurred in S_{-1}. Addition of high concentrations of Ca^{2+} can displace Mn(II) from native binding sites to cause an inhibition of O_2 evolution activity. In contrast to these results, modeling of data from NH_2OH-treated PSII centers incubated in the absence of EDTA did not require an assumption of inactive S_{-1} centers (Figure 5C, Figure 4B, closed symbols) to fit the data. These findings indicate that substantial concentrations of intact PSII centers may exist in a metastable S_{-1} state after treatment with NH_2OH, and these centers can photoactivate rapidly to evolve oxygen. On the other hand, modeling of these data required the assumption that centers reduced to S_{-3} were inactive, in contrast to the observation of O_2 formation from this state that was observed in NH_2-NH_2-treated intact thylakoid membranes (*28*). It is likely that Mn(II) remains trapped in thylakoids where it can be photoactivated, unlike the case in isolated PSII, where the OEC is not sequestered in the thylakoid lumen. At the same time, simulations of these data (Figure 5D and Figure 4B, open symbols) do not adequately account for the excess loss of O_2 evolution activity and Mn(II) that occurs in the range of 3−5 mol of NH_2OH/mol of PSII. High ionic strength causes loss of the 17 kDa and 23 kDa polypeptides from NH_2OH treated PSII samples (*39*), and binding of the extrinsic 33 kDa manganese stabilizing protein has also been proposed to be weakened in NH_2OH-reduced PSII centers (*39*). It is therefore possible that the combined effects of polypeptide release and exposure of the Mn cluster to elevated concentrations of Ca^{2+} are responsible for the increased losses of activity and Mn(II) that are associated with these samples. Support for this proposal comes from the results of experiments in which SWPSII samples were exposed to the conditions used for an intact PSII sample in Figure 5C. Maximum inhibition of O_2 evolution and complete release of Mn(II) occurred in these samples at 2−3 mol of NH_2OH/mol of PSII (data not shown), which would also be consistent with the proposal that the extrinsic 17 and 23 kDa polypeptides stabilize the Mn cluster in PSII centers undergoing photoactivation (*56*, *57*).

A comparison of the data on Mn(II) release from PSII after H_2Q and NH_2OH treatment reveals an interesting contrast in the action of the two reductants. In the case of H_2Q, treatments with EDTA or Ca^{2+} during or after reductant incubations of SWPSII produce, at most, the release of about 3 Mn(II) per PSII reaction center (Figures 2 and 3). For the experiments with intact PSII using NH_2OH as the reductant, it is clear from the data in Figure 5 that exposure of these samples to EDTA or Ca^{2+} can cause the release of nearly 100% of the Mn from these PSII centers. The major difference between these reductants, revealed in the data of Figure 6, is the greater extent of $Y_D^•$ reduction by NH_2OH during long-term incubations. Redox reactions between $Y_D^•$ and the S_0 Mn cluster have been demonstrated (*9*, *58*), and other research has provided evidence for a role of the tyrosine radical in ligation of Mn(II) during assembly and photoactivation of the Mn cluster (*59*). It is therefore possible that that extensive reduction of $Y_D^•$ is responsible for the additional Mn(II) loss detected in samples reduced by NH_2-OH.

In conclusion, the reductant/PSII stoichiometries reported here are consistent with proposals that the S_1 state of the PSII Mn cluster contains 6 oxidizing equivalents. This assignment is consistent with a $Mn(III)_2Mn(IV)_2$ oxidation state, and is in agreement with the oxidation state assignments obtained from XANES data, and from a number of simulations of the S_2 EPR multiline signal. The data also provide evidence in addition to the results in refs *20*, *28*, and *30* that, in intact PSII, reduced states of the Mn cluster can be reactivated by illumination to evolve molecular oxygen. These reduced S states may contain Mn(II) that can be displaced by Ca^{2+} at high concentrations of the latter metal atom, thus eliminating the possibility of reactivation of the OEC by illumination. Finally, the results presented here reveal an additional effect of the extrinsic 23 and 17 kDa polypeptides, which is to promote retention of Mn(II) atoms that would otherwise dissociate from their binding sites in the OEC.

ACKNOWLEDGMENT

We thank Prof. Roseanne Sension for generous assistance in the use of her Monte Carlo simulation program. We are grateful for the helpful comments of the reviewers of this manuscript.

REFERENCES

1. Bricker, T. M., and Ghanotakis, D. F. (1996) Introduction to Oxygen Evolution and the Oxygen-Evolving Complex, in *Oxygenic Photosynthesis: The Light Reactions* (Ort, D. R., and Yocum, C. F., Eds.) Vol. 4, pp 113−136, Kluwer Academic Publishers, Dordrecht, The Netherlands.
2. Britt, R. D. (1996) Oxygen Evolution, in *Oxygenic Photosynthesis: The Light Reactions* (Ort, D. R., and Yocum, C. F., Eds.) Vol. 4, pp 137−164, Kluwer Academic Publishers, Dordrecht, The Netherlands.
3. Kok, B., Forbush, B., and McGloin, M. (1970) Cooperation of charges in photosynthetic O_2 evolution: 1. A linear 4 step mechanism, *Photochem. Photobiol. 11*, 457−475.

4. Forbush, B., Kok, B., and McGloin, M. (1971) Cooperation of charges in photosynthetic O_2 evolution. 2. Damping of flash yield oscillation, deactivation, *Photochem. Photobiol. 14*, 307−321.
5. Miyao, M., and Murata, N. (1985) The Cl^- effect on photosynthetic oxygen evolution—interaction of Cl^- with 18-kDa, 24-kDa and 33-kDa proteins, *FEBS Lett. 180*, 303−308.
6. Miyao, M., Fujimura, Y., and Murata, N. (1988) Partial degradation of the extrinsic 23 kDa protein of the photosystem-II complex of spinach, *Biochim. Biophys. Acta 936*, 465−474.
7. Miyao, M., and Murata, N. (1984) Calcium ions can be substituted for the 24-kDa polypeptide in photosynthetic oxygen evolution, *FEBS Lett. 168*, 118−120.
8. Chu, H. A., Nguyen A. P., and Debus, R. J. (1995) Amino acid residues that influence the binding of manganese or calcium to photosystem-II. 1. The lumenal interhelical domains of the D1 polypeptide, *Biochemistry 34*, 5839−5858.
9. Styring, S., and Rutherford, A. W. (1987) In the oxygen-evolving complex of photosystem-II the S_0 state is oxidized to the S_1 state by D^+ (signal-II slow), *Biochemistry 26*, 2401−2405.
10. Yachandra, V. K., Sauer, K., and Klein, M. P. (1996) Manganese cluster in photosynthesis: Where plants oxidize water to dioxygen, *Chem. Rev. 96*, 2927−2950.
11. Riggs, P. J., Mei, R., Yocum, C. F., and Penner-Hahn, J. E. (1992) Reduced derivatives of the manganese cluster in the photosynthetic oxygen-evolving complex, *J. Am. Chem. Soc. 114*, 10650−10651.
12. Dismukes, G. C., and Siderer, Y. (1981) Intermediates of a polynuclear manganese center involved in photosynthetic oxidation of water, *Proc. Natl. Acad. Sci. U.S.A. 78*, 274−278.
13. Zheng, M., and Dismukes, G. C. (1992) Photosynthetic water oxidation: What have we learned from the multiline EPR signals? in *Research in Photosynthesis* (Murata, N., Ed.) Vol. II, pp 305−308, Kluwer Academic Publishers, Dordrecht, The Netherlands.
14. Zheng, M., and Dismukes, G. C. (1996) Orbital configuration of the valence electrons, ligand field symmetry, and manganese oxidation states of the photosynthetic water oxidizing complex: Analysis of the S_2 state multiline EPR signals, *Inorg. Chem. 35*, 3307−3319.
15. Peloquin, J. M., Campbell, K. A., Randall, D. W., Evanchik, M. A., Pecoraro, V. L., Armstrong, W. H., and Britt, R. D. (2000) Mn-55 ENDOR of the S_2-state multiline EPR signal of photosystem II: Implications on the structure of the tetranuclear Mn cluster, *J. Am. Chem. Soc. 122*, 10926−10942.
16. Peloquin, J. M., and Britt, R. D. (2001) EPR/ENDOR characterization of the physical and electronic structure of the OEC Mn cluster, *Biochim. Biophys. Acta 1503*, 96−111.
17. Carrell, T. G., Tyryshkin, A. M., and Dismukes, G. C. (2002) An evaluation of structural models for the photosynthetic water-oxidizing complex derived from spectroscopic and X-ray diffraction signatures, *J. Biol. Inorg. Chem. 7*, 2−22.
18. Sivaraja, M., and Dismukes, G. C. (1988) Binding of hydroxylamine to the water-oxidizing complex and the ferroquinone electron-acceptor of spinach photosystem-II, *Biochemistry 27*, 3467−3475.
19. Yocum, C. F., Yerkes, C. T., Sharp, R. R., Blankenship, R. E., and Babcock, G. T. (1981), Stoichiometry, inhibitor sensitivity, and organization of manganese associated with photosynthetic oxygen evolution, *Proc. Natl. Acad. Sci. U.S.A. 78*, 7507−7511.
20. Bouges, B. (1971) Action of low concentrations of hydroxylamine on oxygen evolved by chlorella and spinach chloroplasts, *Biochim. Biophys. Acta 234*, 103−112.
21. Förster, V., and Junge, W. (1985) Cooperative and reversible action of 3 or 4 hydroxylamine molecules on the water-oxidizing complex, *FEBS Lett. 186*, 153−157.
22. Förster, V., and Junge, W. (1986) On the action of hydroxylamine, hydrazine and their derivatives on the water-oxidizing complex, *Photosynth. Res. 9*, 197−210.
23. Nugent, H. A., Muhiuddin, I. P., and Evans, C. W. (2003) Effect of hydroxylamine on photosystem II: Reinvestigation of electron paramagnetic resonance characteristics reveals possible S state intermediates, *Biochemistry 42*, 5500−5507.
24. Beck, W. F., and Brudvig, G. W. (1987) Reactions of hydroxylamine with the electron-donor side of photosystem-II, *Biochemistry 26*, 8285−8295.
25. Beck, W. F., and Brudvig, G. W. (1988) Resolution of the paradox of ammonia and hydroxylamine as substrate-analogs for the water-oxidation reaction catalyzed by photosystem-II, *J. Am. Chem. Soc. 110*, 1517−1523.
26. Messinger, J., Nugent, J. H. A., and Evans, M. C. W. (1997) Detection of an EPR multiline signal for the S_0 state in photosystem II, *Biochemistry 36*, 11055−11060.
27. Messinger, J., Roblee, J. H., Wa, O. Y., Sauer, K., Yachandra, V. K., and Klein, M. P. (1997) The S_0 state of the oxygen-evolving complex in photosystem II is paramagnetic: Detection of EPR multiline signal, *J. Am. Chem. Soc. 119*, 1349−11350.
28. Messinger, J., Seaton, G., Wydrzynski, T., Wacker, U., and Renger, G. (1997) S_{-3} state of the water oxidase in photosystem II, *Biochemistry 36*, 6862−6873.
29. Sarrou, J., Isgandarova, S., Kern, J., Zouni, A., Gernot, R., Lubitz, W., and Messinger, J. (2003) Nitric oxide-induced formation of the S_{-2} state in the oxygen-evolving complex of photosystem II from Synechococcus elongatus, *Biochemistry 42*, 1016−1023.
30. Mei, R., and Yocum, C. F. (1992) Comparative properties of hydroquinone and hydroxylamine reduction of the Ca^{2+}-stabilized O_2-evolving complex of photosystem-II—reductant-dependent Mn^{2+} formation and activity inhibition, *Biochemistry 31*, 8449−8454.
31. Ghanotakis, D. F., Topper, J. N., Babcock, G. T., and Yocum, C. F. (1984) Structural and catalytic properties of the oxygen-evolving complex. Correlation of polypeptide and manganese release with the behavior of Z^+ in chloroplasts and a highly resolved preparation of the PSII complex. *Biochim. Biophys. Acta 765*, 388−398.
32. Ono, T.-a., Nouguchi, T., Inoue, Y, Kusunoki, M., Matsushita, T., and Oyanagi, H. (1992) X-ray-detection of the period-4 cycling of the manganese cluster in photosynthetic water oxidizing enzyme, *Science 258*, 1335−1337.
33. Yachandra, V. K., DeRose, V. J., Latimer, M. J., Mukuji, I., Sauer, K., and Klein, M. P. (1993) Where plants make oxygen—a structural model for the photosynthetic oxygen-evolving manganese cluster, *Science 260*, 675−679.
34. Peloquin, J. M., and Britt, R. D. (2001) EPR/ENDOR characterization of the physical and electronic structure of the OEC Mn cluster, *Biochim. Biophys. Acta 1503*, 96−111.
35. Berthold, D. A., Babcock, G. T., and Yocum, C. F. (1981) A highly resolved, oxygen-evolving photosystem-II preparation from spinach thylakoid membranes: Electron-paramagnetic resonance and electron-transport properties, *FEBS Lett. 134*, 231−234.
36. Switala, J., and Lowen, P. C. (2002) Diversity of properties among catalases. *Arch. Biochem. Biophys. 401*, 145−154.
37. Johnson, D. P. (1968) Spectrophotometric determination of oximes and unsubstituted hydroxylamine, *Anal. Chem. 40*, 646−648.
38. Tamura, N., Inoue, H., and Inoue, Y. (1990) Inactivation of the water oxidizing complex by exogenous reductants in PSII membranes depleted of extrinsic proteins, *Plant Cell Physiol. 31*, 469−477.
39. Kavelaki, K., and Ghanotakis, D. F. (1991), Effect of the manganese complex on the binding of the extrinsic proteins (17-kDa, 23-kDa and 33-kDa) of photosystem-II, *Photosynth. Res. 29*, 149−155.
40. Hind, G., and Nakatani, H. Y. (1970) Determination of the concentration and the redox potential of cytochrome 559, *Biochim. Biophys. Acta 216*, 223−225.
41. Cramer, W. A., Fan, H. N., and Bohme, H. (1971) High and low potential states of the chloroplast cytochrome b-559 and thermodynamic control of non-cyclic electron transport, *Bioenergetics 2*, 289−303.
42. Ghanotakis, D. F., Yocum, C. F., and Babcock, G. T. (1986) ESR spectroscopy demonstrates that cytochrome b559 remains low potential in Ca^{2+}-reactivated, salt-washed PSII particles, *Photosynth. Res. 9*, 125−134.
43. Hasegawa K., Kusunoki M., Inoue Y., and Ono T. A. (1998) Simulation of S_2 state multiline EPR signal in oriented photosystem II membranes: Structural implications for the manganese cluster in an oxygen-evolving complex, *Biochemistry 37*, 9457−9465.
44. Kusunoki, M., Ono, T., Noguchi, T., Inoue, Y., and Oyanagi, H. (1993) Manganese K-edge X-ray-absorption spectra of the cyclic S-States in the photosynthetic oxygen-evolving system, *Photosynth. Res. 38*, 331−339.
45. Cooper, S. R., Dismukes, G. C., Klein, M. P., and Calvin, M. J. (1978) Mixed-valence interactions in di-mu-oxo bridged manganese complexes—Electron paramagnetic resonance and magnetic-susceptibility studies, *J. Am. Chem. Soc. 100*, 7248−7252.
46. Hagen, K. S., Armstrong, W. H., and Hope, H. (1988) Isolation of a bis-oxo-bridged Mn-III Mn-IV intermediate by regulated air oxidation—synthesis, structure, and properties of $[Mn_2O_2(Tren)_2](CF_3SO_3)_3$, *Inorg. Chem. 27*, 967−969.

47. Fronko, R. M., Penner-Hahn, J. E., and Bender, C. J. (1988) Electron-paramagnetic resonance spectral evidence for a dinuclear active-site in the Lactobacillus-plantarum manganese catalase, *J. Am. Chem. Soc. 110*, 7554−7555.
48. Kim, D. H., Britt, R. D., Klein, M. P., and Sauer, K. (1990) The g = 4.1 EPR signal of the S_2 state of the photosynthetic oxygen-evolving complex arises from a multinuclear Mn cluster. *J. Am. Chem. Soc. 112* (25), 9389−9391.
49. Kim, D. H., Britt, R. D., Klein, M. P., and Sauer, K. (1992) The manganese site of the photosynthetic oxygen-evolving complex probed by EPR spectroscopy of oriented photosystem-II membranes−the g = 4 and g = 2 multiline signals, *Biochemistry 31*, 541−547.
50. Ghosh, M. C., Reed, J. W., Bose, R. N., and Gould, E. S. (1994) Electron-transfer. 118. Proton-coupled reductions of a dinuclear dimanganese (III, IV) model for the reactive center in photosystem-II, *Inorg. Chem. 33*, 73−78.
51. Shaikh, N., Ali, M., and Banerjee, P. (2002) Kinetic studies on the oxidation of dihydroxybenzenes by monomeric manganese (III)- and bis(mu-oxo) manganese (III, IV)-cyclam complexes−phosphate inhibition, *Inorg. Chim. Acta 339*, 341−347.
52. Messinger, J., Wacker, U., and Renger, G. (1991) Unusual low reactivity of the water oxidase in redox state S_3 toward exogenous reductants. Analysis of the NH_2OH- and NH_2NH_2-induced modifications of flash-induced oxygen evolution in isolated spinach thylakoids, *Biochemistry 30*, 7852−7862.
53. Hanssum, B., and Renger, G. (1985) Studies on the interaction between hydroxylamine and hydrazine as substrate-analogs and the water-oxidizing enzyme system in isolated spinach-chloroplasts, *Biochim. Biophys. Acta 810*, 225−234.
54. Wieghardt, K. (1984) Mechanistic studies involving hydroxylamine, *Adv. Inorg. Bioinorg. Mech. 3*, 213−273.
55. Banerjee, S., Choudhury, U. R., Banerjee, R., and Mukhopadhyay, S. (2002) Kinetic and mechanistic studies on the oxidation of hydroxylamine by a tri-bridged manganese(IV, IV) dimer in weakly acidic media, *J. Chem. Soc., Dalton Trans. 9*, 2047−2052.
56. Ono, T.-A., Kajikawa, H., and Inoue, Y. (1986) Changes in protein composition and Mn abundance in photosystem II particles on photoactivation of the latent O_2-evolving system in flash-grown wheat leaves, *Plant Physiol. 80*, 85−90.
57. Becker, D. W., Callahan, F. E., and Cheniae, G. M. (1985) Photoactivation of NH_2OH-treated leaves: Reassembly of release extrinsic PSII polypeptides and religation of Mn into the polynuclear Mn catalyst of water oxidation, *FEBS Lett. 192*, 209−214.
58. Vass, I., and Styring, S. (1991) pH-dependent charge equilibria between tyrosine-D and the S-states in photosystem II. Estimation of relative midpoint redox potentials, *Biochemistry 30*, 830−839.
59. Ananyev, G. A., Sakiyaw, I., Diner, B. A., and Dismukes, G. C. (2002) A functional role for tyrosine-D in assembly of the inorganic core of the water oxidase complex of photosystem II and the kinetics of water oxidation, *Biochemistry 41*, 974−980.

BI048460I